

Short Communication

Shape optimization of noise barriers using genetic algorithms

D. Duhamel*

*LAMI—unité mixte ENPC/LCPC, Institut Navier, 6 et 8 Avenue Blaise Pascal, Cité Descartes,
Champs sur Marne, 77455 Marne la Vallée, cedex 2, France*

Received 7 April 2005; received in revised form 16 March 2006; accepted 10 April 2006
Available online 12 June 2006

Abstract

This article presents a method to find optimal shapes for noise barriers by coupling a boundary element solution of the sound pressure around the barrier and an optimization process by genetic algorithms to minimize the sound pressure level in a domain behind the barrier. The objective is not to provide geometries with immediate practical applications but to estimate the improvement that could be obtained if noise barriers with improved shapes were used instead of the traditional barriers built today. The method supposes given source and receiver positions and the calculation provides an optimal shape for the barrier to reduce the sound pressure at receiver points over a specified frequency band. Different examples are presented to estimate the influence of the source and receiver positions, of the frequencies and the influence of the size of the barrier. The main conclusion is an estimate of the potential improvement of noise barriers efficiency by using better geometries.

© 2006 Elsevier Ltd. All rights reserved.

1. Introduction

To reduce the noise in the vicinity of roads, one usually builds noise barriers to protect buildings behind the barrier. The design of efficient barriers able to substantially reduce the noise is thus an important question in environmental noise protection. It is well known that the position and the geometry of the barrier, mainly its height, are important parameters to estimate the efficiency of the barrier. However, for aesthetic or practical reasons, it is not suitable to build barriers of very large heights. Thus, for improving barrier efficiencies, it is necessary to design new shapes and covering of barriers to try to improve their performances for a given total height.

Several authors have addressed these questions from an experimental or a numerical point of view. For barriers with complex shapes which cannot be calculated by analytical methods, Sez nec [1] proposed to develop calculations by the boundary element method (BEM) to estimate their efficiency with precision. Then, Hothersall et al. [2,3] calculated the performances of various noise barriers by two-dimensional (2D) boundary elements. They studied a range of barrier forms including straight, circular, Y and T shapes and different surface coatings and found that a T shape can provide clear improvements in barrier efficiency in the shadow zone. In Ref. [4], numerical calculations and scale model studies of multiple noise barriers were obtained and it

*Tel.: +33 1 64 15 37 28; fax: 33 1 64 15 37 41.
E-mail address: duhamel@lami.enpc.fr.

was found that multiple barriers also provide a significant improvement over single barriers. Other studies comparing various barriers were also done by Ishizuka and Fujiwara [5] for a large range of shapes.

Many experimental studies were also done to estimate the influence of barrier shapes on their performances. In Ref. [6] scale models were used to experimentally test various noise barrier shapes and the authors in Ref. [7] calculated and also tested with scale models different straight, circular and T shape barriers with reactive surfaces. Both found that some shapes, for instance the T shape with absorbent covering, provide clear improvement over straight barriers. Full scale tests were conducted by Watts et al. [8], Watts [9], and Watts and Morgan [10] to compare the efficiency of T shape, multiple edge barriers and double barriers. An improvement from 1 to 3 dB over simple plane reflective barriers of identical height was found.

Finally, Shao et al. [11] and Ho et al. [12] proposed noise barriers with random edge profiles to decrease the coherence in the diffracted sources. They obtained some improvements over a traditional straight barrier especially at high frequencies. Experiments were also done on random edge noise barriers and an improvement was found except for low frequencies.

In these earlier studies, the authors proposed different barrier shapes with or without covering materials and they tested their efficiency by numerical calculations or by doing experiments. For improving the efficiency they try to imagine different shapes, for instance by changing the top of the barrier and then they estimate experimentally the benefit obtained in noise reduction. However, these approaches suffer from the lack of a systematic method to obtain good shapes.

In this work, we propose a different approach by coupling a BEM with a genetic algorithm optimization process to obtain improved geometries. In the first part of the article we outline the techniques of the BEM and the optimization by genetic algorithms. Then we present some examples of calculation for different configurations. The objective of this article is not really to provide optimal geometries with immediate practical applications but rather to estimate the potential improvement in noise barrier efficiency that can be obtained by using better geometries than the conventional ones.

2. Calculation of optimal shapes

2.1. Sound pressure calculation

The problem that we are studying in this article is described in Fig. 1 where a noise barrier of arbitrary shape is presented. We consider only the 2D case which is sufficient if we study only propagation paths normal to the barrier. In Ref. [13], it was shown that 2D and 3D calculations of noise barriers lead to the same insertion loss for a normal propagation. A source radiates noise on one side of the barrier and the objective is to reduce the sound pressure level on the other side. In this article, to simplify and to enlighten the effect of barrier shapes, the ground and the barrier are supposed rigid. The sound pressure around the barrier for harmonic waves with the time dependence $e^{-i\omega t}$ is the solution of the Helmholtz equation

$$\nabla^2 p(x, \omega) + k^2 p(x, \omega) = s(x, \omega), \quad (1)$$

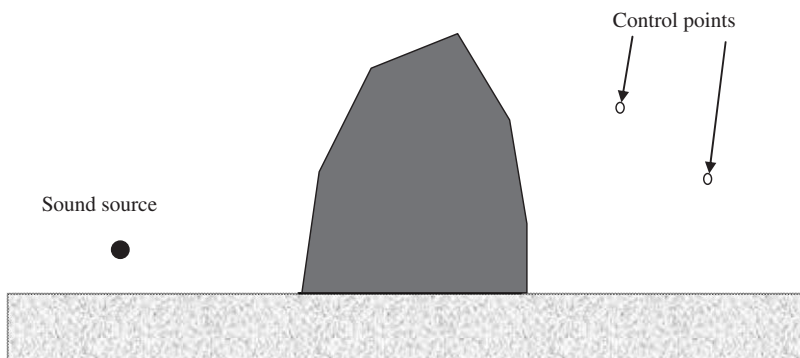


Fig. 1. Noise barrier of complex shape.

where p is the sound pressure at point x and for frequency ω , $k = \omega/c$ is the wave number, c is the sound velocity and $s(x, \omega)$ is the source term in the fluid medium which for a point source of amplitude A at x_s equals $-A\delta(x-x_s)$. In the following unit amplitude is used. As the barrier and the ground are rigid the sound pressure is such that the normal derivative equals zero on the barrier and on the ground:

$$\frac{\partial p}{\partial n} = 0. \quad (2)$$

Moreover the sound pressure is such that the Sommerfeld condition is satisfied at infinity:

$$\lim_{r \rightarrow \infty} \left(\frac{\partial p}{\partial r} - ikp \right) = o\left(\frac{1}{\sqrt{r}}\right). \quad (3)$$

For barriers with complex shapes the pressure can be calculated by the BEM. Details on calculations by BEMs can be found in Refs. [13–15]. As is well known, the BEM suffers from nonuniqueness of the solution at a discrete set of frequencies. These are associated with the resonance frequencies of the domain interior to the barrier. The problem can be solved by the Burton and Miller formulation [16], which consists in solving another equation obtained by taking the usual boundary integral equation plus its normal derivative multiplied by a complex constant. Details on the precise form of the BEM used here can be found in Ref. [17].

2.2. Genetic algorithms and cost functions

In the following we are interested in minimizing the sound behind the barrier. So our cost function is

$$J = 10 \log_{10} \left[\frac{1}{n_p n_f} \sum_{i=1}^{n_f} \sum_{j=1}^{n_p} |p(x_j, \omega_i)|^2 \right]. \quad (4)$$

This is the value in decibels of the average of the square of the sound pressure over a number n_p of points behind the barrier and over n_f frequencies. Changing the number of points can lead to small or large control zones behind the barrier. The number of frequency points can lead to a control over a wide band of frequencies for n_f large or at a unique frequency if $n_f = 1$.

As J can be a very complicated function of the barrier shape, of the frequency and of the control points, and since it can only be estimated numerically, a sophisticated optimization process is necessary. Genetic algorithms are optimization algorithms used for solving complex problems associated with cost functions having many local minima. A general description of genetic algorithms can be found in Refs. [18,19]. This method is a direct optimization method which means that it only needs the evaluation of the function without requiring its derivatives. This is well adapted to our problem because the derivative of the cost function (4) is complicated to calculate. The mathematical problem is to find the minimum of a cost function J with real values defined on a parameter set. The parameters are coded as finite-length strings over some finite alphabet. For the present problem a parameter is a shape for the barrier with the constraint of being included in a rectangle to avoid too large barriers.

The coding process is obtained by approximating the geometry of the barrier by small rectangles which can be filled by matter (1) or can be empty (0). An example is given in Fig. 2. So the geometry is coded by a rectangular matrix of zeros and ones. Then from such a matrix of zeros and ones, one has to define the geometry of the barrier. The first step is to remove the interior holes which are not connected to the fluid domain. Then the boundary of each connected domain defines the barrier boundary, a detailed example is given in Fig. 3. It is then meshed by usual techniques of the BEM. The mesh is made with quadratic three nodes elements which were found to provide a better precision than linear two nodes elements. Each elementary rectangular part of the shape (a 1 in the 0/1 coding) is meshed with 8 elements per wavelength of the highest frequency tested, here 2000 Hz. Then a computation by the BEM and a simple post-processing of the results allow calculating the cost function (4). This provides a value of the cost function J for each matrix of zeros and ones produced by the genetic algorithm.

Genetic algorithms define crossing, mutations and selections on a set of individuals. At each generation the individuals reproduce, survive or disappear according to the values of the cost function of each individual. At

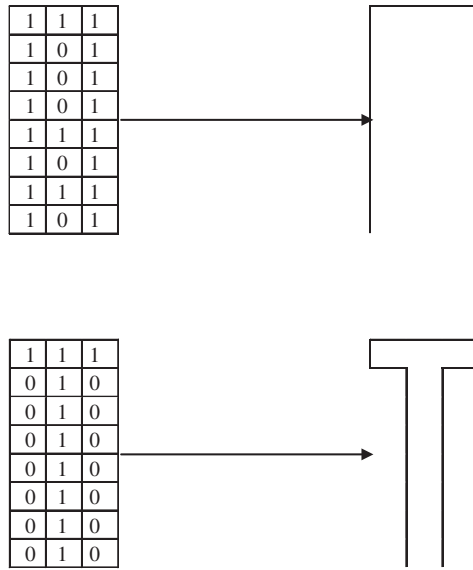


Fig. 2. Building of the geometry from binary data.

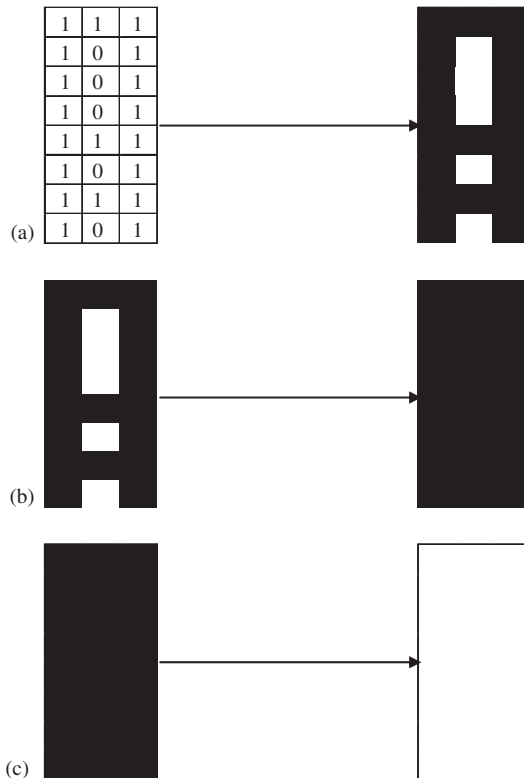


Fig. 3. Example for a rectangular barrier: (a) fill the 1 in the matrix to build the first step of the geometry, (b) remove the interior holes and (c) build the boundary of the domains.

each step the algorithm selects which individual can reproduce and which individual disappears such that the size of the population is constant. The creation of new individuals from the current population and the evolution of populations can be obtained from two processes: crossing and mutation. In the crossing process

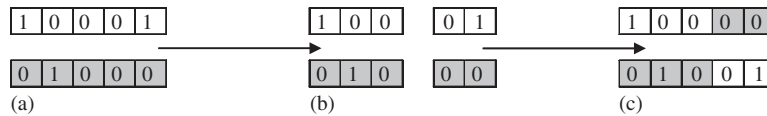


Fig. 4. One point crossing of two genotypes with (a) the original two chromosomes, (b) the splitting of the two chromosomes and (c) the two final chromosomes obtained by exchanging the second parts shown in (b).

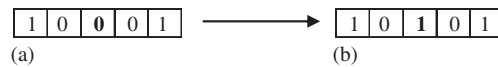


Fig. 5. Example of mutation operator by changing third bit: (a) before mutation and (b) after mutation.

presented in Fig. 4, from two parents, a new individual is obtained by cutting the chromosome at a random location and exchanging the two parts. The crossing rate defines which proportion of the population is submitted to this operation. Tests on this parameter were made between 0.60 and 0.90. The results show that a parameter between 0.7 and 0.8 leads to interesting convergence rates which are stable over different runs while other values can be good on a run and very bad for another. In the following examples this parameter is set to 0.75. The second operator is the mutation which is a random exchange between 0 and 1 on the bits of the chromosomes with a small probability, see Fig. 5 for an example. The mutation rate was tested between 0.001 and 0.05. Too large values must be avoided because they lead to poor convergence. In the following this parameter equals 0.002. These operators avoid a stagnation of the algorithm on local minima and allow a global search of the optimum. The population size was set to 10. Increasing this number could give better results but at the price of much longer computing times. After the mutation process the best individuals are kept to form the new population. At each generation 25% of the individuals are replaced. In the calculation presented here the C++ library Galib [20] is used and more specifically the GA2DBinarystring class which is well adapted for a chromosome described by a matrix of zeros and ones.

3. Results

3.1. Efficiency of straight and T shape barriers

As a basis for a comparison with the following calculations, the sound pressure for a straight wall of width 0.1 m and for a T shape wall is calculated. These walls are presented in Fig. 6. The origin of the coordinate system is defined at the bottom centre of the barrier. The sound source is located at point $(-5 \text{ m}, 0)$ on the ground and it radiates the pressure $iA/4H_0(kr)$ in free field. The sound velocity is 340 m/s. We are interested by the sound pressure behind the barrier and we define the zone 1 by the five points given in Table 1. This is a square zone of area 0.25 m^2 , see Fig. 6. A second and larger zone, denoted zone 2, is defined in Table 2 with 20 points.

The values of the cost functions for the straight and T shape barriers are given in Table 3. The function J_{125} is the cost function defined by formula (4) for the frequency 125 Hz, while J_{2000} is the same for the frequency 2000 Hz and $J_{125-2000}$ is the cost function obtained by taking the average on the five frequencies 125, 250, 500, 1000 and 2000 Hz in formula (4). The T shape wall is a little more efficient than the straight wall by 1 to 3 dB depending on the frequency. The average level in zone 2 is a little larger than in zone 1, which seems quite reasonable as much more points are involved in the calculation of the cost function.

3.2. Convergence of the algorithm

We first test the convergence of the genetic algorithm. The barrier is defined from a mesh of 5×20 rectangles inside the rectangular domain such that $-0.25 \text{ m} \leq x \leq 0.25 \text{ m}$ and $0 \text{ m} \leq y \leq 2 \text{ m}$. Each elementary rectangle can be filled or empty as explained previously. A computation is done with 1000 iterations for the cost functions at 125 and 2000 Hz and with 500 iterations for the cost function including the five frequencies

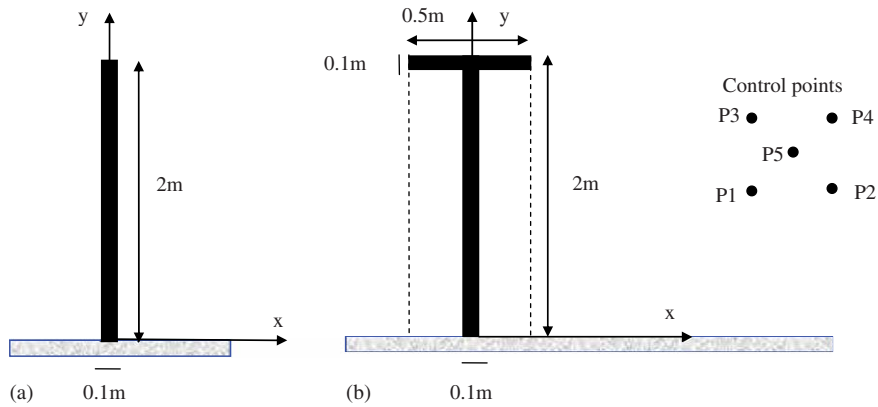


Fig. 6. Straight and T shape barriers.

Table 1
Coordinates of the points defining the zone 1

Points	P1	P2	P3	P4	P5
X(m)	2	2.5	2	2.5	2.25
Y(m)	1	1	1.5	1.5	1.25

Table 2
Coordinates of the points defining the zone 2

Points	P1	P2	P3	P4	P5	P6	P7	P8	P9	P10
X(m)	2	3	4	5	2	3	4	5	2	3
Y(m)	0	0	0	0	0.5	0.5	0.5	0.5	1	1
Points	P11	P12	P13	P14	P15	P16	P17	P18	P19	P20
X(m)	4	5	2	3	4	5	2	3	4	5
Y(m)	1	1	1.5	1.5	1.5	1.5	2	2	2	2

Table 3
Cost functions for the reference walls relative to the values for the straight barrier with zone 1

	J (dB) zone 1	J (dB) zone 2
Straight wall 125 Hz, J_{125}	0	+ 2.4
Straight wall 2000 Hz, J_{2000}	0	+ 1.3
Straight wall 125–2000 Hz, $J_{125-2000}$	0	+ 1.6
T wall 125 Hz, J_{125}	-0.9	+ 0.5
T wall 2000 Hz, J_{2000}	-3.0	-0.4
T wall 125–2000 Hz, $J_{125-2000}$	-1.8	-0.5

125, 250, 500, 1000 and 2000 Hz. The evolution of the cost function for five runs with different initial seeds is presented in Fig. 7. To avoid a too complex figure only the best and worst values of the cost function are presented at each step. One can see a rapid decrease of the cost function during the first 100 iterations and a slower decrease after. The final values of the cost functions for each case are given in Table 4. The dispersion between the different runs is rather important. It is about 2 dB except for 2000 Hz where it reaches 5 dB. From these results, one can see that it is better to do several computations to get a reasonable estimate of the best configuration for each problem.

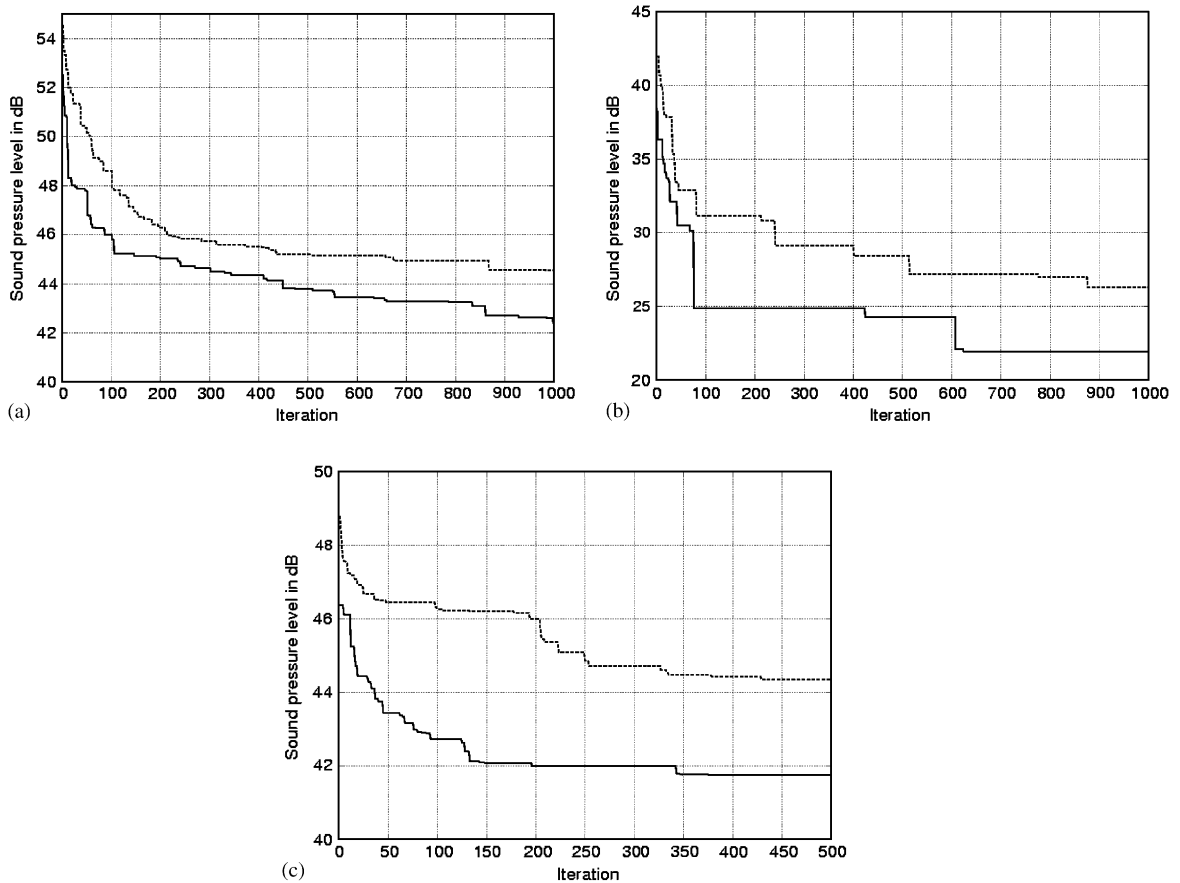


Fig. 7. Evolution of the sound pressure level for the best and worse cases on five runs with the iteration number for the frequencies 125 Hz (a), 2000 Hz (b) and for 125–2000 Hz (c); — best value for five runs, - - - - - worse value for five runs.

Table 4

Cost functions relative to the values for the straight wall for 5 runs after 1000 iterations for 125 and 2000 Hz and after 500 iterations for the band 125–2000 Hz

	J_{125} (dB)	J_{2000} (dB)	$J_{125-2000}$ (dB)
Optimization 1	-14.3	-7.6	-9.6
Optimization 2	-12.8	-12.0	-9.8
Optimization 3	-12.2	-9.0	-8.5
Optimization 4	-13.5	-8.1	-7.5
Optimization 5	-13.4	-8.5	-10.0
Best	-14.3	-12.0	-10.0

From the curve presenting the cost function for the five frequencies between 125 and 2000 Hz, one observes that the cost function does not change a lot after 300 iterations. For the calculation at 125 and 2000 Hz the larger decrease in the sound pressure level is also obtained after 300 iterations. To save computing time, the following calculations will be stopped after 300 iterations. Of course this value is arbitrary and is only defined as a compromise between the quality of the result and the computing time.

In Fig. 8, computations are made for the frequencies 500 and 2000 Hz to test the influence of the number of runs. The minimum of the cost function is presented for five and ten runs. Very little differences can be seen

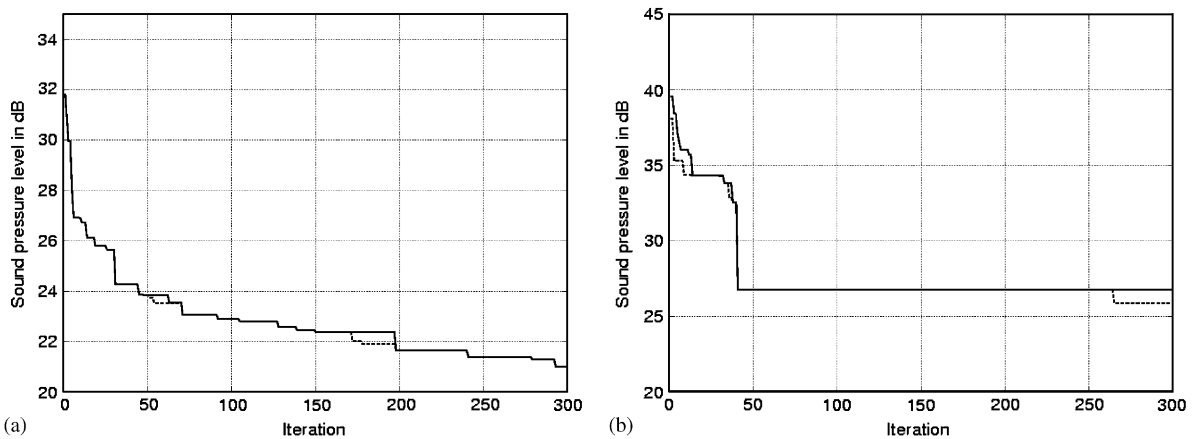


Fig. 8. Minimum values of the cost functions: (a) frequency 500 Hz and (b) frequency 2000 Hz with: — minimum for five runs, ---- minimum for 10 runs.

between the two curves. So it seems that doing five runs is quite sufficient to have a good estimate of the minimum of the cost function.

3.3. Shapes of the barriers

The final shapes of the best barriers for the frequencies 125, 2000 Hz and for the band 125–2000 Hz are presented in Fig. 9. It can be seen that the shapes are complex and quite different with the frequency. They can also be multiconnected with holes inside. Such shapes would be difficult to obtain with simpler optimization methods relying on continuous displacements of some points on the boundary of the walls. If we look at the shape of the top of the barrier, it seems in Fig. 9b and c that interference effects between the different parts of the barrier should be responsible for the improvement of this barrier over conventional ones. On the contrary at 125 Hz in Fig. 9a the shape of the top of the barrier is simple as we cannot expect interesting interferences at this frequency.

From these results it can be seen that gains of about 14 dB at 125 Hz and 12 dB at 2000 Hz are obtained for the control zone 1 if we compare to the sound pressure level of a straight barrier (see Table 4). A decrease of 10 dB relative to the straight barrier can also be observed in the frequency band 125–2000 Hz. So it seems possible to build a barrier much more efficient than the usual ones for a large frequency band.

3.4. Influence of the size of the control zone and of the barrier

In Fig. 10 the results for the cost function $J_{125-2000}$ for the control zone 2 are presented. The final value of the cost function for the best run is 46.3 dB. In the case of a control in zone 1, the final value was about 41.8 dB. So the increase in the size of the control zone leads to a loss of 4.5 dB in the average sound pressure. For the T shape barrier this final value was 51.3 dB. The result of the shape optimization of the barrier is still a gain of 5 dB over the T shape.

The final shape of the barrier for the best run is presented in Fig. 11. It looks like the complex shapes of Fig. 9. A comparison of the sound pressure near the barrier for a T shape and for the optimal shape is given in Fig. 12. It can be observed a decrease in sound pressure level behind the barrier of about 5 dB as indicated by the value of the cost function. The black part of the figure indicates the zone where the optimal shape has reduced the sound pressure level by about 8 dB in comparison with the T shape. One can see that the zone where the sound pressure level has been reduced includes most of the zone behind the barrier showing that the new shape is efficient on a zone of significant size and is not limited to the points where the control is done. The shape of the barrier includes a lonely square on the left side. A computation was made with this square omitted. The value of the cost function is 46.3 dB with the initial geometry and 46.9 dB with the square omitted. So the difference between the two cases is small. However, a closer look at the results show that the

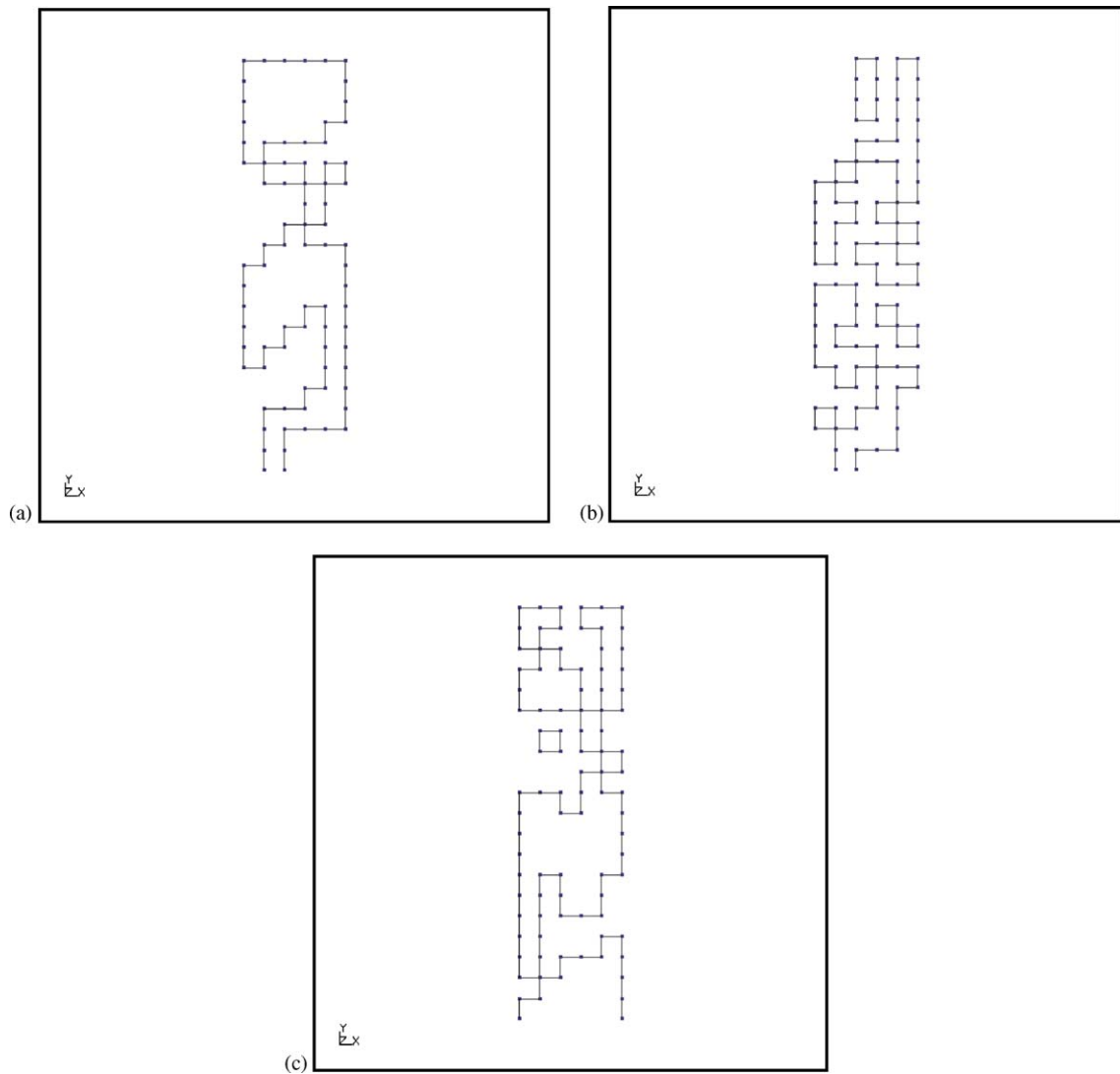


Fig. 9. Final shapes of the barriers for the best runs and for the frequencies 125 Hz (a), 2000 Hz (b) and for 125–2000 Hz (c).

difference in sound pressure level is very small for the frequencies 100, 250, 500 and 1000 Hz while it is 8 dB for 2000 Hz. So the lonely square acts by improving the diffraction at 2000 Hz and has no influence for the other frequencies.

Another computation is made for a barrier meshed with 8×20 rectangles over the rectangular surface such that $-0.4 \text{ m} \leq x \leq 0.4 \text{ m}$ and $0 \text{ m} \leq y \leq 2 \text{ m}$, which is a little larger than before. The results are presented in Fig. 13 for the frequency band 125–2000 Hz and the control zone 1. The final value of the cost function is 44.9 dB which is not better than for the smaller size of the barrier where it was 41.8 dB. So it seems that increasing the horizontal size of the barrier decreases the convergence speed of the algorithm rather than improving the final result.

3.5. Position of the source

As a final test, the barrier in Fig. 11 is calculated for other positions of the source to see if the optimal shape for a position of the source and a control zone is still interesting for other positions of the source. The cost

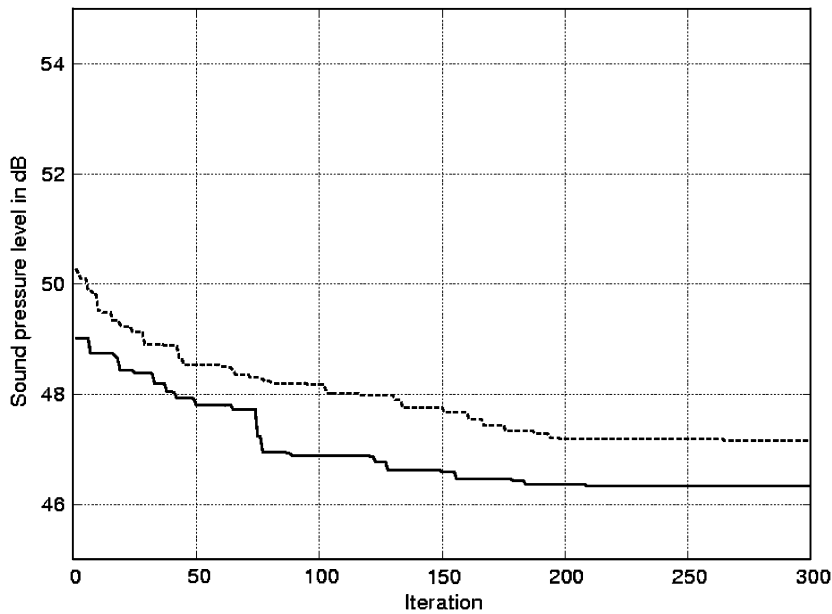


Fig. 10. Evolution of the sound pressure level with the iteration number for the frequencies 125–2000 Hz and the control zone 2; — best value for five runs, ----- worse value for five runs.

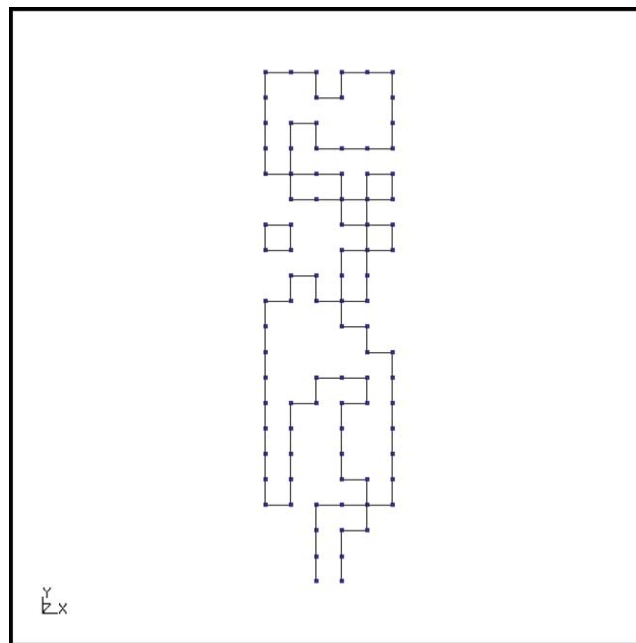


Fig. 11. Optimal shape for the frequencies 125–2000 Hz and the control zone 2.

function $J_{125-2000}$ is used with the control zone 2. The sound source is now positioned at $(-3, 0.5)$ and then at $(-7, 0.1)$. The values of the cost function for the T shape and for the shape of Fig. 11 for these three positions of the sound source are given in Table 5. It can be seen that the optimal shape is better than the straight shape for the three sound source positions by at least 7 dB. So the optimal shape of a barrier found for a source position can also be interesting for a large set of source positions.

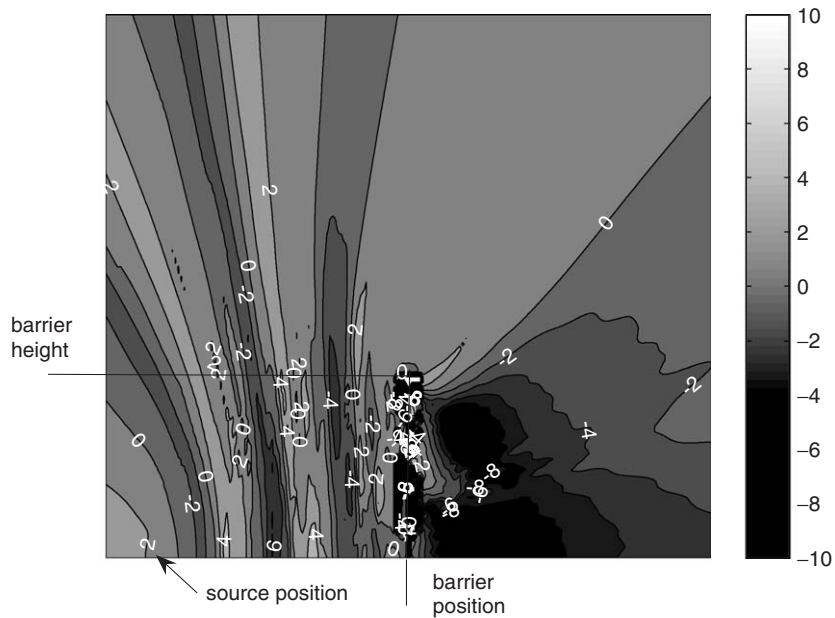


Fig. 12. Difference between the sound pressure levels for the optimal barrier and the T shape barrier for the frequencies 125–2000 Hz and the control zone 2. The black zones are the domains where the sound pressure level is reduced by using the optimal shape. The source is on the ground at 5 m on the left of the barrier.

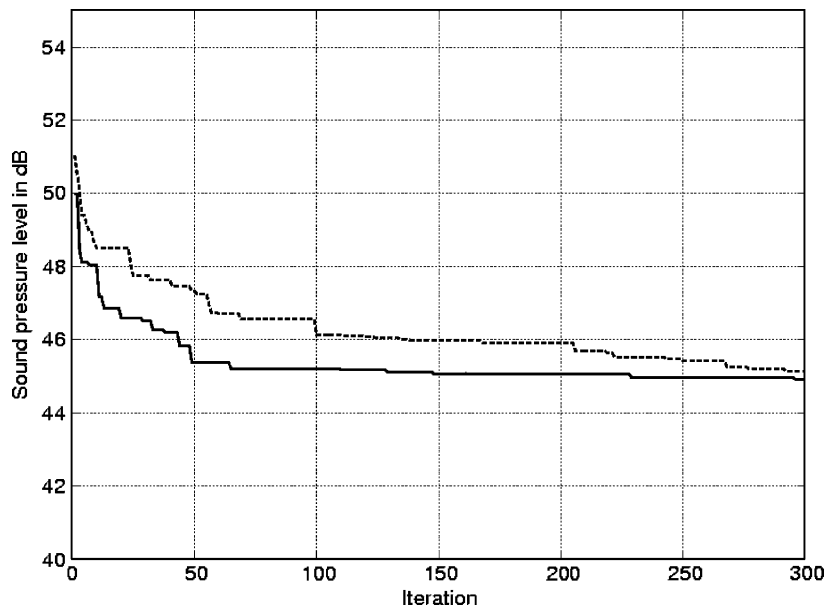


Fig. 13. Evolution of the sound pressure level with the iteration number for the frequencies 125–2000 Hz and a large barrier: — best value for five runs, - - - - worse value for five runs.

4. Conclusions

An optimization method based on a coupled BEM and genetic algorithm was built to find optimal noise barrier shapes. Interesting results can be obtained in some hundred steps of the genetic algorithm. Complex shapes were obtained which could be difficult to build in a practical application. However, the most interesting

Table 5
Cost functions for T and optimal shapes for different sound source positions

	$J_{125-2000}$ (dB)
T shape, source position 1 (−5,0)	−2.1
T shape, source position 2 (−3,0.5)	−4.6
T shape, source position 3 (−7,0.1)	−2.6
Optimal shape, source position 1 (−5,0)	−7.0
Optimal shape, source position 2 (−3,0.5)	−9.4
Optimal shape, source position 3 (−7,0.1)	−7.5

The values are given relatively to the straight wall with the source position (−5, 0).

fact in these results is the proof that the attenuation obtained with traditional straight or T shape noise barriers seems far from optimal. At least a further 5 dB in efficiency could be obtained by a better design of the barrier. This study was done for rigid barriers and only the shape was optimized but of course the covering of the barrier could also be optimized in a future study to get still better results. Practical realizations would also need an improved cost function to avoid the generation of barriers with too complex shapes.

References

- [1] R. Seznec, Diffraction of sound around barriers: use of the boundary elements technique, *Journal of Sound and Vibration* 73 (1980) 195–209.
- [2] D.C. Hothersall, S.N. Chandler-Wilde, M.N. Hajmirzae, Efficiency of single noise barriers, *Journal of Sound and Vibration* 146 (1991) 303–322.
- [3] D.C. Hothersall, D.H. Crombie, S.N. Chandler-Wilde, The performance of T-profile and associated noise barriers, *Applied Acoustics* 32 (1991) 269–287.
- [4] D.H. Crombie, D.C. Hothersall, The performance of multiple noise barriers, *Journal of Sound and Vibration* 176 (1994) 459–473.
- [5] T. Ishizuka, K. Fujiwara, Performance of noise barriers with various edge shapes and acoustical conditions, *Applied Acoustics* 65 (2004) 125–141.
- [6] D.N. May, M.M. Osman, Highway noise barriers: new shapes, *Journal of Sound and Vibration* 71 (1980) 73–101.
- [7] K. Fujiwara, D.C. Hothersall, C. Kim, Noise barriers with reactive surfaces, *Applied Acoustics* 53 (1998) 255–272.
- [8] G.R. Watts, D.H. Crombie, D.C. Hothersall, Acoustic performance of new designs of traffic noise barriers: full scale test, *Journal of Sound and Vibration* 177 (1994) 289–305.
- [9] G.R. Watts, Acoustic performance of a multiple edge noise barrier profile at motorway sites, *Applied Acoustics* 47 (1996) 47–66.
- [10] G.R. Watts, P.A. Morgan, Acoustic performance of an interference-type noise-barrier profile, *Applied Acoustics* 49 (1996) 1–16.
- [11] W. Shao, H.P. Lee, S.P. Lim, Performance of noise barriers with random edge profiles, *Applied Acoustics* 62 (2001) 1157–1170.
- [12] S.S.T. Ho, I.J. Busch-Vishniac, D.T. Blackstock, Noise reduction by a barrier having a random edge profile, *Journal of the Acoustical Society of America* 101 (1997) 2669–2676.
- [13] D. Duhamel, Efficient calculation of the three-dimensional sound pressure field around a noise barrier, *Journal of Sound and Vibration* 197 (1996) 547–571.
- [14] M. Bonnet, *Boundary Integral Equation Methods for Solids and Fluids*, Wiley, New York, 1999.
- [15] R.D. Ciskowski, C.A. Brebbia, *Boundary Element Methods in Acoustics*, Elsevier, Amsterdam, 1991.
- [16] A.J. Burton, G.F. Miller, The application of integral equation methods to the numerical solution of some exterior boundary value problems, *Proceedings of the Royal Society of London A* 323 (1971) 201–210.
- [17] A. Fadavi, *Modélisation numérique des vibrations d'un pneumatique et de la propagation du bruit de contact*, PhD thesis, ENPC, 2002.
- [18] J.H. Holland, *Adaptation in natural and artificial systems*, The University of Michigan Press, 1975.
- [19] D.E. Goldberg, *Genetic Algorithms in Search, Optimization, and Machine Learning*, Addison-Wesley, Reading, MA, 1989.
- [20] GALib, A C++ Library of Genetic Algorithm components <http://lancet.mit.edu/ga/>.